The Magnetic Booster Target Inertial Confinement Fusion Driver

F. Winterberg

Desert Research Institute, University of Nevada System, Reno, Nevada 89507, USA

Z. Naturforsch. **39 a,** 325 – 341 (1984); received October 24, 1983

A promising candidate for a near-term low-cost inertial confinement fusion driver is the magnetic booster target concept. In it a small high density magnetically confined plasma and which serves as booster stage, is compressed and ignited by hypervelocity impact. The energy released in the magnetic booster stage, after being transformed into black body radiation, ablatively implodes a high gain second stage target and which releases most of the thermonuclear energy. Alternatively, the energy released in the booster stage can be also used to compress and ignite a target as in impact fusion. The importance of this concept is that it permits to drive the booster stage with a mass accelerator at a velocity of a few 10 km/sec, which is small compared to the velocity required for pure impact fusion, even though it is more than one order of magnitude larger than what can be directly reached with ordinary guns or high explosives. The required velocities can probably be reached by magnetic guns and by fluid dynamic methods through the implosion of cylindrical or spherical shells driven by light gas gun fired projectiles. In comparison to laser- or charged particle beam drivers, the initial driver power is several orders of magnitude smaller and which should lead to a substantial reduction in the driver cost.

1. Introduction

The principal problem of inertial confinement fusion is not the modest amount of driver energy, estimated to be in between 1 and 10 MJ, but the requirement that this energy be delivered in less than 10 ns to a target less than 1 cm^2. This imposes on all drivers so far experimentally or theoretically studied, and which are beams ranging from photons (lasers) over electrons, light and heavy ions up to macroscopic projectiles, very severe conditions at the limit of technical feasibility. As a consequence all these different driver concepts are very expensive. Expressing the driver cost in \$/Joule, a glass laser with $\sim 10^3$ \$/Joule is at the top and would become prohibitively expensive if an energy of a few megajoule is required. The cheapest drivers presently studied, with a cost of \$ 10/J, are intense ion beams produced in magnetically insulated high voltage diodes, a concept proposed by the author many years ago [1]. The impact fusion approach to inertial confinement, requiring the acceleration of macroparticles to several 100 km/sec, may lead to an even lower driver cost, provided however, that certain technical problems can be solved *.

In Table 1 the estimated costs for the different driver options, under the assumption that a trigger energy of about 5×10^6 J is required, are summarized.

In an attempt to reduce the driver costs substantially, an entirely new driver approach had been proposed and which the author has called the magnetic booster target inertial confinement fusion driver [4, 5, 6].

The idea to use strong magnetic fields in inertial confinement fusion targets, both to trap the fusion α-particles and to reduce the heat conduction losses, has been considered previously [1] and has been revived more recently [7]. The magnetic booster target concept however, goes far beyond the mere suggestion to utilize a magnetic field in inertial confinement fusion targets. Superficially it combines magnetic with inertial fusion. More specifically, it combines three branches of controlled fusion research and which are 1) magnetic fusion, 2) impact fusion and 3) inertial fusion. For two specific magnetic confinement configurations, a linear z- and a θ-pinch, the idea is explained in Figure 1. In both cases, a small cm-size magnetically confined plasma, and which is the booster stage, is imploded by hypervelocity impact, if it is placed on a anvil hit by a hypervelocity projectile. By the implosive compression through the hypervelocity impact, the magnetized plasma is isentropically compressed and thereby heated until it reaches the ignition temperature for thermonuclear reactions to take place.

* Some reduction of the required velocity is possible if upon impact the projectile generates and compresses black body radiation which thereafter ablatively implodes a target [2, 3].

Reprint requests to Prof. F. Winterberg, Desert Research Institute, University of Nevada System, Reno, Nevada 89507/USA.

0340-4811 / 84 / 0400-0325 \$ 01.3 0/0. – Please order a reprint rather than making your own copy.

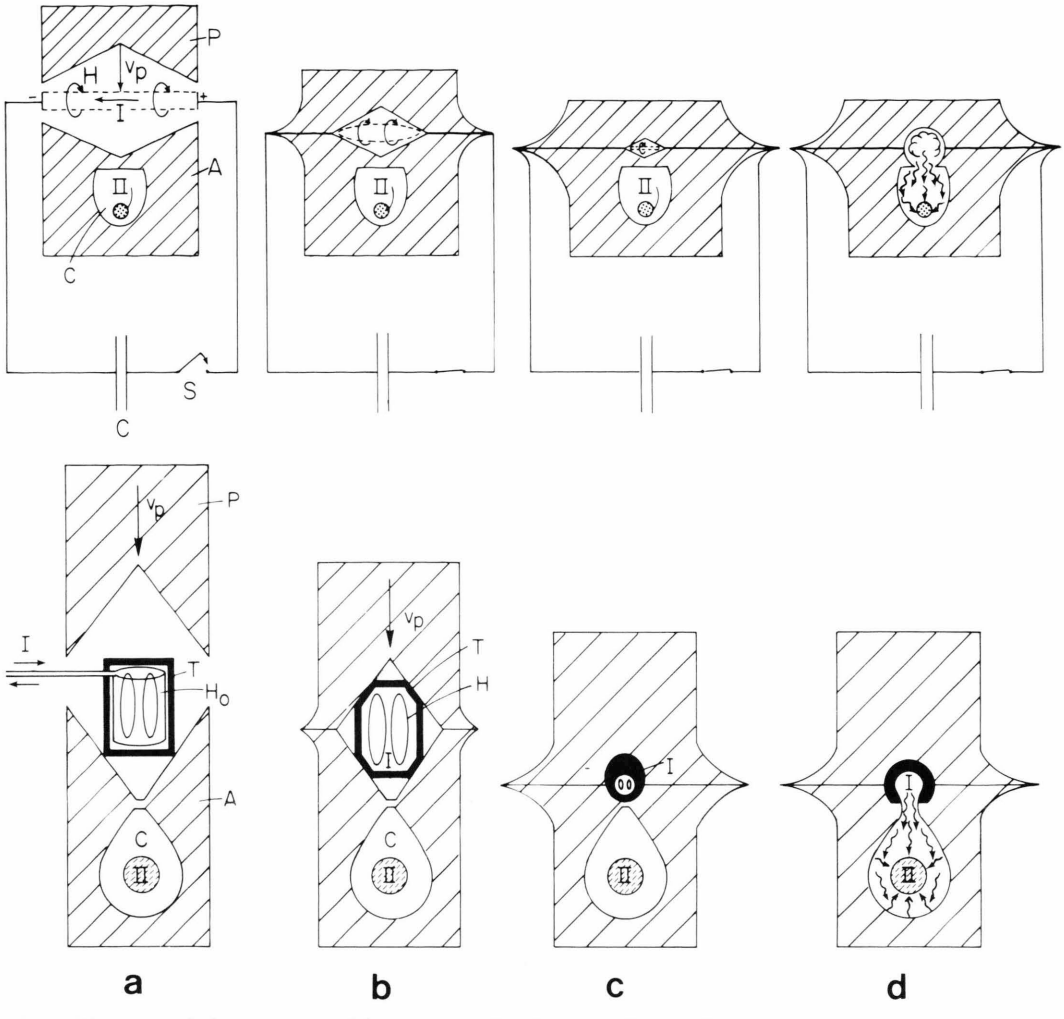

Fig. 1. The magnetic booster stage driver concept for the case of a small z-pinch and a small θ-pinch. I magnetic booster stage, II high-gain ablative implosion stage. P projectile, A anvil, I electric current, H_0 initial magnetic field, T tamp.

After ignition the plasma undergoes a thermonuclear excursion and explosively mixes with the wall material, resulting in the generation of intense black body radiation. The thermonuclear burn rapidly increases the pressure in the cavity with the result that a "window", leading to second chamber containing a second stage high yield target, is blown out. The black body radiation from the first chamber of the booster target rushes through the blown out window into the second chamber and where it ablatively implodes the second stage high yield target. In this configuration the overwhelming part of the thermonuclear energy is released in the second stage. The first or magnetic booster stage serves here primarily as a power amplifier to drive the second stage. Because the booster stage can be imploded by a driver of much less power than the power required to drive the second high gain stage, a much cheaper primary driver can be used. This becomes apparent if one realizes that the booster stage can be driven by a projectile or a mass accelerated to a few 10 km/sec, a velocity which can probably be reached by magnetic guns and even by combination of light gas gun fired projectiles and imploding shells. By comparison, the velocities needed for pure impact fusion, which are almost 10 times larger, are much more difficult to reach. This fact gives the magnetic booster stage concept its

Table 1. Cost of beam type inertial confinement fusion drivers.

Driver	Glas laser	Gas laser	Heavy ion beam	Light ion beam	Macroparticle, magnetic travelling wave
Cost \$/Joule	10^3	10^2	10^2	10	1
Cost for 5×10^6 J in \$	5×10^9	5×10^8	5×10^8	5×10^7	5×10^6

decisive advantage not only over pure impact fusion concepts, but over all other driver options.

Another no less important fact is that unlike magnetically confined fusion plasmas working at manageable pressures and which not only must be magnetohydrodynamically stable, but also stable against microinstabilities, the magnetic booster stage plasma can tolorate microinstabilities and hence can work even with Bohm diffusion losses, because of the much higher plasma density of the booster stage, typically 10^6 times larger. In low density magnetic fusion plasmas Bohm diffusion must be prevented if the plasma and hence confinement apparatus shall be kept within reasonable dimensions. The booster stage is magnetohydrodynamically stabilized by the conducting wall of the imploded cavity. This stabilizes even the small imploded z-pinch shown in Figure 1. With wall stabilization only perturbations with a wavelength much shorter than the diameter of the cavity can have an influence and which are much less important.

The booster stage has great similarity to the fast liner approach by Linhart [8], except that in the fast liner approach a magnetically confined plasma is compressed by the implosion of a thin cylindrical shell, which is driven by magnetic forces, by letting a large axial current pass along its surface. To obtain a high liner velocity requires a thin shell, but if a dense magnetic fusion plasma shall serve as a booster stage to ignite a second high yield stage, the shell must be sufficiently fat. If this condition is not met, the confinement time is too short and not enough fusion energy can be released from the booster stage to ignite the second stage. In the magnetic booster concept the liner must be a thick projectile or large mass accelerated to a few 10 km/sec. One possibility by which this could be done is a magnetic macroparticle accelerator. It has the distinct advantage that it permits to feed the energy into the projectile rather slowly. This means that the power needed to drive the accelerator can be even lower than the already much lower power required to drive the booster stage. However, in order to make the accelerator as short as possible one may wish to accelerate the projectile with the highest possible acceleration compatible with its tensile strength. If the acceleration is a [cm/sec^2], the tensile strength of the projectile is σ [dyn/cm^2] and ϱ its density one has

$$a \leqq \sigma/(\varrho\, h), \tag{1.1}$$

where h the height of the projectile. The length L of the accelerator to reach a velocity v is then given by

$$L = v^2/2\, a = \varrho\, v^2 h/2\, \sigma. \tag{1.2}$$

Typically one has $\sigma \simeq 10^{10}$ dyn/cm^2. For $\varrho = 7$ g/cm^3 (iron) and $h \simeq 1$ cm one finds that $a \leqq 1.43 \times 10^9$ cm/sec^2. If, for example, $v = 40$ km/sec, one finds $L = 56$ meter. However, as we show below $h \simeq 4$ cm is a more likely value for which $L \simeq 225$ meters. Two accelerators, each producing $v = 20$ km/sec would then have a combined length of ~ 100 meters.

The power to drive the macroparticle accelerator is given by

$$P = \sqrt{a/2L}\; E = aE/v, \tag{1.3}$$

where E is the projectile energy in erg. Assuming that $E = 10^7$ Joule $= 10^{14}$ erg, $v = 2 \times 10^6$ cm/sec, and $a \simeq 1.43 \times 10^9$ cm/sec^2 one finds $P \simeq 7 \times 10^{16}$ erg/sec $= 7 \times 10^9$ Watt. This power is about five orders of magnitude smaller than the power needed for beam driven inertial confinement fusion concepts. Since the energy in \$/Joule rises sharply with the driver power, it is to be expected that this enormous reduction in the primary driver power must be accompanied by a very large reduction in the driver cost.

The idea to replace the liner in Linhart's approach with a fast moving projectile accelerated by a macroparticle accelerator was proposed by Ribe and Vlases [9]. These authors, however, did not propose to use the thusly formed dense magnetic

fusion plasma as a booster stage to drive an inertial confinement fusion target. It is only through this combination of magnetic and inertial fusion that very high gains can be expected.

Another possibility to reach the required velocities is through fluiddynamic methods. This would have the advantage that the limitation for the attainable acceleration given by (1.1) does not apply and the length over which to accelerate can there become much shorter.

Rather than to drive ablatively a second stage target by the black body radiation from the booster stage, one may instead use the high velocity generated by the exploding booster stage and which is imparted on the tamp, to drive an impact fusion target. A configuration of this kind using a z-pinch booster stage is shown in Figure 2. In comparison to an ablatively imploded second stage, the attainable densities are here smaller and correspondingly the thermonuclear yield, but this alternative concept may therefore also have a better chance to succeed.

2. The Booster Stage

To obtain the scaling laws of the booster stage we assume that the booster stage plasma has the linear dimension l and is imploded three-dimensionally. This means, for example, that in the case of a z-pinch booster, the pinch is compressed both radially and axially.

In the absence of energy losses, the temperature of the imploding plasma rises as

$$T/T_0 = (l_0/l)^{3(\gamma-1)}, \tag{2.1}$$

where γ is the specific heat ratio of the imploded plasma. For $\gamma = 5/3$, valid for a DT plasma, one has

$$T/T_0 = (l_0/l)^2. \tag{2.2}$$

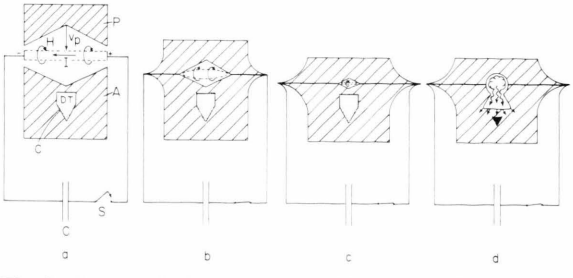

Fig. 2. Impact fusion target making use of magnetic booster stage.

Under the assumption that the cavity wall is a good conductor, the magnetic field is trapped within and rises as

$$H/H_0 = (l_0/l)^2. \tag{2.3}$$

The electric current in the cavity, which includes both the surface current along the cavity wall and the current passing through the plasma, rises as

$$I/I_0 = l_0/l. \tag{2.4}$$

The current density $j \simeq (H/l)$ [A/cm^2], rises as

$$j/j_0 = (l_0/l)^3, \tag{2.5}$$

the particle number density rises as

$$n/n_0 = (l_0/l)^3, \tag{2.6}$$

and the plasma pressure as

$$p/p_0 = (l_0/l)^5. \tag{2.7}$$

Finally, the β-value, that is the ratio of the plasma pressure to the magnetic pressure rises as

$$\beta/\beta_0 = l_0/l. \tag{2.8}$$

The values T_0, H_0, I_0, j_0, n_0, p_0 and β_0 are the values of T, H, I, j, n, p and β for $l = l_0$.

To reduce end losses, the magnetic field lines must be closed. In a z-pinch and in a field reversed θ-pinch the field lines are already closed. However, even in a configuration where the field lines are initially open the currents induced in the imploding plasma and the cavity wall result in eventual field reversal, no matter what the initial field distribution is. Field reversal occurs approximately if the magnetic field strength has doubled. Calling the value of l where field reversal occurs l_r, then according to (2.3), putting $H = 2H_0$, one finds that

$$l_r \simeq l_0/\sqrt{2}\,. \tag{2.9}$$

The cavity of the booster stage typically implodes to a minimum diameter $l_{min} \sim l_0/10$. Field reversal therefore takes place at an early stage of the implosion. From there on the field lines are closed and the end losses are eliminated.

At $l = l_{min}$, reached at the maximum state of implosion, the maximum temperature T_{max} must reach the ignition temperature for the thermonuclear reaction.

From (2.2) one has

$$\frac{1}{T}\frac{\mathrm{d}T}{\mathrm{d}t} = -\frac{2}{l}\frac{\mathrm{d}l}{\mathrm{d}t}. \tag{2.10}$$

Introducing the projectile velocity v_p

$$v_p = -\,\mathrm{d}l/\mathrm{d}t, \tag{2.11}$$

this is

$$\frac{1}{T}\frac{\mathrm{d}T}{\mathrm{d}t} = \frac{2}{l}v_p. \tag{2.12}$$

From (2.12) one obtains the characteristic adiabatic rise time τ_A of the temperature in the booster stage cavity, which, if it implodes from $l = l_0$ to $l = l_{min} \ll l_0$, is

$$\tau_A = l_0/2\,v_p. \tag{2.13}$$

This time has to be smaller than both the loss time τ_R for bremsstrahlung and τ_c for heat conduction. Otherwise the adiabatic assumption for the temperature rise, (2.2), becomes invalid. To obtain an upper estimate for these losses we evaluate them at $l = l_{min}$ where $T = T_{max}$, $n = n_{max}$ and $H = H_{max}$. The loss time for bremsstrahlung is given by

$$\tau_R = 3 \times 10^{11}\, T_{max}^{1/2}/n_{max} \quad [\mathrm{sec}], \tag{2.14}$$

and the loss time for heat conduction in the presence of a strong transverse magnetic field by

$$\tau_c = 1.7\,(l_{min}\,H_{max})^2\,T_{max}^{1/2}/n_{max} \quad [\mathrm{sec}]. \tag{2.15}$$

To compute the impact pressure we note that for velocities for which

$$(1/2)\,\varrho_p\,v_p^2 \gg \sigma, \tag{2.16}$$

where ϱ_p is the density of the projectile and σ its tensile strength, the projectile must be viewed as a fluid. For iron $\varrho_p \simeq 7\ \mathrm{g/cm^3}$ and $\sigma \simeq 10^{10}\ \mathrm{dyn/cm^2}$, therefore $(1/2)\,\varrho_p\,v_p^2 > \sigma$ for $v_p \geqq 0.5$ km/sec. Since our impact velocity is a few 10 km/sec, the projectile impact must be therefore viewed as the impact of a fluid. Assuming that this fluid is incompressible, its impact pressure p_s upon hitting an infinitely rigid wall is given by Bernoulli's equation:

$$p_s = (1/2)\,\varrho_p\,v_p^2. \tag{2.17}$$

This expression becomes invalid for stagnation pressures $p_s > \varkappa^{-1}$, where $\varkappa = (1/\varrho_0)\,\partial\varrho/\partial p$ is the compressibility of the projectile material. If this material is steel one has $\varkappa = 6 \times 10^{-13}\ \mathrm{cm^2/dyn}$ and the incompressibility assumption becomes invalid for $v_p \geqq 8$ km/sec.

With an equation of state of the form [10]

$$p = A\,\varrho^{\gamma} \tag{2.18}$$

one can use the theory of plane shocks [11] to obtain the stagnation pressure. In (2.18) $A = A(s)$ depends on the entropy of the shock-comressed material. Furthermore, the specific heat ratio γ is a slowly varying function of p. For steel at megabar pressures $\gamma \simeq 10$, but for higher pressures γ becomes smaller and for very high pressures reaches asymptotically the value $\gamma = 5/3$, valid for an monatomic ideal gas or a Fermi gas. Data obtained from high explosive experiments suggest for intermediate pressures that $\gamma \simeq 4$.

If, as before, the projectile makes an impact onto an infinitely rigid wall, we may view this event in the reference system of the wall. In this frame the projectile makes an impact with the velocity v_p onto the wall and as a result a shock wave moves into the projectile with the velocity

$$v_s = \frac{(\gamma+1)}{2}\,v_p. \tag{2.19}$$

The pressure p_s behind a strong shock wave is given by

$$p_s = \frac{2}{\gamma+1}\,\varrho_p\,v_s^2, \tag{2.20}$$

which, if expressed by v_p, is

$$p_s = \frac{\gamma+1}{2}\,\varrho_p\,v_p^2. \tag{2.21}$$

In (2.21) ϱ_p is the density in front of the shock wave and which is equal to the uncompressed projectile mass density. If $\gamma \simeq 10$, p_s would be 11 times larger than for an incompressible projectile, and even for $\gamma = 5/3$, p_s would still be about $8/3 \sim 3$ times larger. In reality, the pressure is only 1/4 as large, because the projectile collides with a nonrigid wall having approximately the same compressibility as the projectile itself. To obtain some reasonable estimates we therefore can take the Bernoulli value of the stagnation pressure given by (2.17).

If two projectiles collide with the same velocity with each other head on, the pressure would be about 4 times larger. The same should happen in a spherical implosion.

The time the pressure lasts during the state of maximum implosion where $l = l_{min}$ is given by

$$\tau_i \simeq 2\,h/v_p, \tag{2.22}$$

where h is the length of the projectile. This is roughly the time for the shock wave and following

rarefaction wave to pass through the projectile. It is also the inertial confinement time for a substance brought in between the projectile and the wall.

Pressure balance at the state of maximum implosion gives

$$H_{\max}^2/8\,\pi + 2\,n_{\max}\,k\,T_{\max} \leqq (1/2)\,\varrho\,v_p^2. \quad (2.23)$$

Magnetic confinement requires that $\beta \leqq 1$. Assuming that $\beta = 1$, one finds

$$H_{\max} \leqq \sqrt{2\,\pi\,\varrho_p}\,v_p, \quad (2.24)$$

and hence with (2.23)

$$n_{\max} \leqq \frac{\varrho_p\,v_p^2}{8\,k\,T_{\max}}. \quad (2.25)$$

Prior to its implosion the plasma must be preheated and provided with an initial magnetic field. At the beginning of the implosion process the magnetic field diffuses into the DT gas resulting in breakdown and Joule heating. An upper limit of the initial plasma temperature T_0, as a result of this Joule heating process, can be obtained by equating the magnetic energy density with the internal energy. This leads to

$$3\,n_0\,k\,T_0 \leqq H_0^2/8\,\pi, \quad (2.26)$$

where H_0 is the initial seed field and n_0 the initial atomic number density of the preheated plasma.

For the initial magnetic field H_0 a current I_0 has to be set up inside the booster stage plasma. This current is of the order

$$I_0 \simeq 5 H_0\,l_0 \quad [\mathrm{A}]. \quad (2.27)$$

After ignition of the booster stage plasma only that part of the thermonuclear energy released as kinetic energy of charged fusion products can contribute to the selfheating of the booster stage plasma, but in addition only if

$$r_L < l_{\min}, \quad (2.28)$$

where r_L is the Larmor radius of the charged fusion products. In case of a DT plasma 80% of the energy released goes into neutron, with the remaining 20% going into α-particles. For the DT reaction the Larmor radius of the fusion α-particles is given by

$$r_L \simeq 2 \times 10^5/H \quad [\mathrm{cm}], \quad (2.29)$$

therefore inequality (2.28) reads

$$H_{\max}\,l_{\min} > 2 \times 10^5 \quad [\mathrm{G\,cm}]. \quad (2.30)$$

Because of its unusual high density the burning plasma can reach the Lawson condition even for Bohm diffusion. The Bohm diffusion time is given by

$$\tau_B \simeq 10^{-4}\,l_{\min}^2\,H_{\max}/T_{\max} \quad [\mathrm{sec}]. \quad (2.31)$$

For $\beta = 1$ one has $H_{\max}^2/8\,\pi = 2\,n_{\max}\,k\,T_{\max}$ and hence

$$\tau_B \simeq 10^{-11}\,l_{\min}^2\,(n_{\max}/T_{\max})^{1/2} \quad [\mathrm{sec}]. \quad (2.32)$$

To satisfy the Lawson criterion under the assumption of Bohm diffusion requires that

$$n_{\max}\,\tau_B \gg n_{\max}\,\tau_L, \quad (2.33)$$

where τ_L is the Lawson time obtained from the Lawson criterion. For the DT reaction $n_{\max}\,\tau_L \gtrsim 10^{14}$ sec/cm^3. Inserting this value into (2.33) together with $T = T_{\max} \simeq 10^8$ K, the ignition temperature of the DT reaction, one obtains

$$n_{\max}\,l_{\min}^{4/3} \gg 2 \times 10^{19} \quad [\mathrm{cm}^{-5/3}]. \quad (2.34)$$

Above thermonuclear ignition always $\tau_R > \tau_L$, because the ignition temperature is defined by $\tau_R = \tau_L$. For an ignited plasma one must, of course, also have $\tau_c > \tau_L$. For $\beta = 1$, that is for $H_{\max}^2/8\,\pi = 2\,n_{\max}\,k\,T_{\max}$ one obtains from (2.15)

$$\tau_c \simeq 1.2 \times 10^{-14}\,T_{\max}^{3/2}\,l_{\min}^2. \quad (2.35)$$

In case of the DT reaction where $T_{\max} \simeq 10^8$ K, the condition $n_{\max}\,\tau_c > n_{\max}\,\tau_L \simeq 10^{14}\,\mathrm{cm}^{-3}\,\mathrm{sec}$, simply yields

$$n_{\max}\,l_{\min} \simeq 10^{16} \quad [\mathrm{cm}^{-2}]. \quad (2.36)$$

The thermonuclear burn excursion lasts the inertial confinement time τ_i given by (2.22). This time has to be compared with the burn-up time τ_f of the thermonuclear fuel. The burn-up time follows from the reaction rate equation, which for two different species of nuclei in a stoechiometric mixture is determined by

$$\frac{\mathrm{d}n}{\mathrm{d}t} = -\frac{n^2}{4}\langle\sigma\,v\rangle, \quad (2.37)$$

where $\langle\sigma\,v\rangle$ is the product of the relative collision velocity and the nuclear reaction cross section averaged over a Maxwellian velocity distribution, and n the atomic number density, counting both species. (If the species are equal the factor 1/2 appears on

the r.h.s. of (2.37) instead of the factor 1/4). Putting $dn/dt = -n_{max}/\tau_f$ and $n = n_{max}$ one obtains

$$\tau_f = 4(n_{max}\langle\sigma v\rangle)^{-1}. \tag{2.38}$$

A large thermonuclear burn-up has taken place provided $\tau_f \sim \tau_i$. The ratio τ_i/τ_f is approximately the burn-up fraction. Equating τ_i with τ_f one obtains a condition for the length h of the projectile giving a large burn-up, and one finds

$$h \sim 2v_p/n_{max}\langle\sigma v\rangle. \tag{2.39}$$

If the energy for a single fusion reaction is given by ε_0 and the fraction of that energy going into charged fusion products f, the energy density ε and hence the pressure in the booster chamber rises during the thermonuclear burn excursion to

$$\varepsilon \sim p \sim f(n_{max}^2/4)\langle\sigma v\rangle \varepsilon_0 \tau_i = f n_{max} \varepsilon_0 (\tau_i/\tau_f). \tag{2.40}$$

During the thermonuclear excursion the pressure thus rises by the factor

$$F \sim f\varepsilon_0 \tau_i/2kT_{max}\tau_f. \tag{2.41}$$

In the special case of the DT reaction $f = 0.2$ and $\varepsilon_0 = 2.8 \times 10^{-5}$ erg and $T_{max} \simeq 10^8$ K, one has

$$F \sim 200\,\tau_i/\tau_f. \tag{2.42}$$

For a 50% fuel burn-up with $\tau_i/\tau_f = 0.5$ one would have $F \sim 100$.

In reaching the ignition temperature $T = T_{max}$ one has $\beta \lesssim 1$, but in the course of the thermonuclear excursion $\beta \sim 100$, since it is proportional to the plasma pressure and hence to F.

The very large rise in β during the thermonuclear excursion means that the hot plasma will hit the cavity wall and ablate some of its material. As long as the ablation is not too large, the energy of the cavity is transformed into black body radiation with a temperature computed from Stefan Boltzmann's law

$$\varepsilon = aT_b^4, \tag{2.43}$$

where $a = 7.67 \times 10^{-15}$ erg/cm^3 K^4.

Let us illustrate the made estimates by a specific example applicable to a DT booster plasma. We choose $v_p = 40$ km/sec and $\varrho_p = 7$ g/cm^3. This velocity is equivalent to two projectiles with $v_p = 20$ km/sec or a shell implosion of the same final speed. Equation (2.17) then gives $p_s \simeq 5.7 \times 10^{13}$ dyn/cm^2, and (2.24) $H_{max} \simeq 2.7 \times 10^7$ G. At ignition where $T = T_{max} \simeq 10^8$ K, (2.25) gives $n_{max} \simeq 10^{21}$ cm^{-3}. This is well above the density given by (2.36) below which heat conduction losses are important.

Let us now assume that $l_0 = 4$ cm and $l_{min} = l_0/10 = 0.4$ cm. If no losses take place then we have for the initial and final values of the booster stage:

$l_0 = 4$ cm,	$l_{min} = 0.4$ cm,
$n_0 = 10^{18}$ cm^{-3},	$n_{max} = 10^{21}$ cm^{-3},
$T_0 = 10^6$ K,	$T_{max} = 10^8$ K,
$H_0 = 2.7 \times 10^5$ G,	$H_{max} = 2.7 \times 10^7$ G,
$I_0 = 6.6 \times 10^6$ A,	$I_{max} = 6.6 \times 10^7$ A,
$j_0 = 5.3 \times 10^4$ A/cm^2,	$j_{max} = 5.3 \times 10^7$ A/cm^2,
$p_0 = 3 \times 10^8$ dyn/cm^2,	$p_{max} = 3 \times 10^{13}$ dyn/cm^2,
$\beta_0 = 0.1$,	$\beta_{max} = 1$.

We note that these values satisfy inequality (2.26) since $3n_0kT_0 \simeq 4 \times 10^8$ erg/cm^3 and $H_0^2/8\pi \simeq 3 \times 10^9$ erg/cm^3. The initial magnetic field H_0 in diffusing into the DT gas should thus be sufficient to preheat it to a temperature of $\sim 10^6$ K.

With $l_0 = 4$ cm and $v_p = 4 \times 10^6$ cm/sec one has from (2.13) $\tau_A \simeq 5 \times 10^{-7}$ sec. With the above given numerical values one has from (2.14) and (2.15) $\tau_R \simeq 3 \times 10^{-6}$ sec and $\tau_c \simeq 2 \times 10^{-3}$ sec. Since τ_R and τ_c have been computed at their maximum values, the assumption that the corresponding losses can be neglected is quite good.

One furthermore has $H_{max} l_{min} = 1.1 \times 10^7$ [G cm], and at $H = H_{max}$, $r_L/l_{min} \simeq 2 \times 10^{-2}$, therefore also condition (2.30) is well satisfied. Finally, one has $n_{max} l_{min}^{4/3} \simeq 3 \times 10^{20}$ [cm$^{-5/3}$], which shows that Bohm diffusion poses no problem.

After ignition the plasma temperature rises until $\langle\sigma v\rangle$ reaches its maximum value. For the DT reaction this is $\langle\sigma v\rangle_{max} \cong 10^{-15}$ cm^3/sec. Using this number one finds from (2.38) that $\tau_f \simeq 4 \times 10^{-6}$ sec. The projectile length to guarantee a large fuel burn-up is then computed from (2.39) to be $h \sim 8$ cm. For two projectiles, or an imploding shell, v_p is only half as large and the same is true for h, which then becomes $h \simeq 4$ cm.

To compute the total amount of fusion energy released we assume a 50% fuel burn-up. The total number of nuclei in a cavity of volume $l_{min}^3 = (0.4)^3$ cm^3 with a number density $n_{max} = 10^{21}$ cm^{-3} is $N = 6.4 \times 10^{19}$. If half of them undergo a fusion reaction, each of which requires two reacting partners, and setting $\varepsilon_0 = 17.6$ MeV $= 2.8 \times 10^{-5}$ erg, the total fusion energy released is

$$E_f = (1/4)\,N\,\varepsilon_0 \simeq 4.5 \times 10^{14} \text{ erg} = 45 \text{ MJ}.$$

The fraction of this energy which goes into the charged α-particles is

$$E_\alpha = 9\ \mathrm{MJ}.$$

At the beginning of the burn, the pressure is $p = p_{\max} \simeq 3\times 10^{13}\ \mathrm{dyn/cm^2}$ and hence the energy density $\varepsilon = (3/2)\, p_{\max} \sim 4\times 10^{13}\ \mathrm{erg/cm^3}$. With a 50% burn-up the pressure and energy density rise to $p \sim 3\times 10^{15}\ \mathrm{dyn/cm^2}$ and $\varepsilon \sim 4\times 10^{15}\ \mathrm{erg/cm^3}$. If this energy is converted into black body radiation, the temperature of this radiation is $T_b \simeq 2.7\times 10^7$ K. The radiation pressure at this temperature is $p_r = a T_b^4/3 \simeq 1.3\times 10^{15}\ \mathrm{dyn/cm^2}$, and the radiation flux

$$\Phi = (a\,c/4)\ T_b^4 \cong 3\times 10^{25}\ \mathrm{erg/cm^2\,sec} = 3\times 10^{18}\ \mathrm{Watt/cm^2}.$$

To estimate how well the radiation is confined by the wall of the imploded cavity, one needs an expression for the average mean free path λ_p of the black body radiation photons. This path length can be obtained from the opacity coefficient [12]

$$\varkappa = 4.34\times 10^{25}\,\varrho\, T^{-3.5}\,(g/t) \quad [\mathrm{cm^2/g}] \tag{2.44}$$

and one has

$$\lambda_p = (\varkappa\,\varrho)^{-1}. \tag{2.45}$$

In (2.44) g and t are called the Gaunt and guillotine factor. For high densities $g \cong 1$. For hydrogen rich stellar atmospheres (Russel mixture) one has $t \cong 10$, but if the wall consists of high Z-number material it is likely that $t \cong 1$. A good approximation for the optical path length is therefore

$$\lambda_p = 2.3\times 10^{-26}\, T^{3.5}/\varrho^2 \quad [\mathrm{cm}]. \tag{2.46}$$

At the high stagnation pressure of $p_s \cong 5.7\times 10^{13}$ dyn/cm^2, the shell material is compressed to a much higher density than under normal conditions. The density can be estimated from an equation of state of the form given by (2.18). To determine the constant A appearing in (2.18) we make the assumption that for $p = p_1 = \varkappa^{-1}$, where $\varkappa$ is the compressibility of the projectile material, $\varrho = \varrho_1 = 2\varrho_p$. One thus has

$$p \cong \frac{1}{2^\gamma\,\varkappa}\left(\frac{\varrho}{\varrho_p}\right)^\gamma. \tag{2.47}$$

Then putting $p = p_s$ one finds

$$\varrho/\varrho_p = 2\,\varkappa^{1/\gamma}\, p_s^{1/\gamma}. \tag{2.48}$$

For the above given value $\gamma \cong 4$ and $\varkappa \cong 6\times 10^{-13}$ cm^2/dyn, one finds

$$\varrho/\varrho_p \cong 1.75\times 10^{-3}\, p_s^{1/4}. \tag{2.49}$$

If $p_s \cong 5.7\times 10^{13}\ \mathrm{dyn/cm^2}$ one has then $\varrho/\varrho_p \cong 4.8$ and for $\varrho_p = 7\ \mathrm{g/cm^3}$ one finds that $\varrho \cong 34\ \mathrm{g/cm^3}$. At this density and at $T = T_b \cong 2.7\times 10^7$ K, the photon mean free path is $\lambda_p \cong 2\times 10^{-3}$ cm. After the material has expanded to its original density $\varrho = \varrho_p$ the mean free path has increased to $\sim 5\times 10^{-2}$ cm.

The photon flux into the wall is given by

$$j = \frac{\lambda_p\, c}{3}\,\frac{\partial}{\partial n}\,(a\,T^4), \tag{2.50}$$

where n is a direction normal to the wall. Putting $j = a\,T^4\,v_d$, where v_d is the photon diffusion velocity, furthermore $\partial\,(a\,T^4)/\partial n \sim a\,T^4/l_{\min}$, one finds that

$$v_d/c \sim (1/3)\,\lambda_p/l_{\min}. \tag{2.51}$$

Therefore, as long as $\lambda_p/l_{\min} \ll 1$ the photons are sufficiently well confined. For our example we have $v_d/c \sim 2\times 10^{-3}$ or $v_d \sim 6\times 10^7$ cm/sec. The confinement time τ_p of the photon gas is

$$\tau_p \sim l_{\min}/v_d = 3\,l_{\min}^2/c\,\lambda_p \tag{2.52}$$

which for our example is $\tau_p \sim 8\times 10^{-9}$ [sec].

An interesting modification of the booster stage arises if both the projectile and anvil consist of fissile material. If, for example, a fissile material is ~ 2 fold compressed, the reaction range of the 14 MeV fusion neutrons released by the booster stage is half as large. The neutron cross section for fission reactions is $\sigma_f \cong 2\times 10^{-24}\ \mathrm{cm^2}$. With $n \cong 2\,n_0 \cong 10^{23}\ \mathrm{cm^{-3}}$, the fission reaction range in the compressed fissile material is $\lambda_F = 1/n\,\sigma_f = 5$ cm. This has about the correct magnitude required by (2.39), if $h \sim \lambda_F$.

In our previous example $N/4 = 1.6\times 10^{19}$ fusion reactions took place producing an equal number of neutrons. Each of these neutrons can now make a fission reaction within a volume of the order $\lambda_F^3 = 125\ \mathrm{cm^3}$. Since each fission reaction sets free $180\ \mathrm{MeV} \cong 2.9\times 10^{-4}$ erg, the total energy set free is equal to $5.0\times 10^{15}\ \mathrm{erg} = 500$ MJ. The energy density in the volume λ_F^3 will be $\varepsilon \sim 4\times 10^{13}\ \mathrm{erg/cm^3}$ and the pressure $p = (2/3)\,\varepsilon \sim 3\times 10^{13}\ \mathrm{dyn/cm^2}$. This pressure though, is about 100 times smaller than the pressure in the booster stage and therefore of little help to enhance the inertial confinement of the booster stage. In this modification and even without

the second high gain stage, the concept may be useful as a hybrid fission-fusion burner. It could, of course, also serve as an efficient fusion induced breeder for the production of fissile material from U 238 or Th 232.

3. The High Gain Main Stage

The high pressure in the booster stage pushes against its confining wall and it should therefore be possible in principle to make the booster stage cavity rupture at a weak point blowing out a hole thereby connecting it with another cavity and into which the second stage high yield target is placed. If, for example, the booster stage cavity has to expand 2-fold in its diameter before the rupture occurs, the black body radiation temperature in the cavity goes down 2-fold, from $T_b \cong 3 \times 10^7$ K to $T_b' \cong 1.5 \times 10^7$ K, and the radiation flux goes down to $\Phi = (a\,c/4)\,T_b'^4 \cong 3 \times 10^{24}$ erg/cm^2 sec $= 3 \times 10^{17}$ W/cm^2. If the blown out opening leading to the cavity containing the second stage target has a cross section of $\sim 10^{-2}$ cm^2, a flux of $\sim 3 \times 10^{15}$ W rushes into this cavity. During the 2-fold expansion of the booster stage cavity one half of the energy goes into work expanding the chamber. Therefore, of the initially 9 MJ energy released inside the booster stage, only 4.5 MJ are available as radiation. At a power level of 3×10^{15} W, the photon flux lasts for $(4.5 \times 10^7)/(3 \times 10^{15}) \cong 10^{-9}$ sec. This time is short compared with the photon confinement time given by (2.52). The second stage will be therefore bombarded more or less uniformly from all sides by the incoming black body radiation.

According to calculations by Bangerter [13], a double shell target with a radius of 0.25 cm, if bombarded with an energy of ~ 2 MJ and a pulse power in excess of 100 TW, produces a ~ 600 fold gain. The surface of Bangerter's target is ~ 1 cm^2, and if the wall of the cavity containing this target has an area ~ 10 times larger than the target itself, the target would be bombarded with $\sim (1/10) \times 3 \times 10^{15}$ Watt ~ 300 TW. Not all of the incident energy will be absorbed by the target, but if the wall of the cavity containing the target consists of dense material, for example gold or uranium, it can have a much higher opacity than the ablator material of the target. As a result a much larger energy fraction per unit area can be absorbed by the target rather than the wall. In our example we assumed that the area of the wall is about 10 times larger. Therefore, the assumption, that about $\sim 1/2$ of the available 4 MJ goes into the target and the other 1/2 into the wall, appears reasonable.

As we had mentioned in the introduction, and as it is illustrated in Fig. 2, instead of driving a second stage target by ablative implosion, one may directly use the kinetic energy of the material from the exploding booster stage to drive an impact fusion target. The kinetic energy density and hence explosion velocity can be estimated by putting

$$\tfrac{1}{2}\varrho_p v_p'^2 \sim \varepsilon\,, \tag{3.1}$$

where ε is the final energy density of the booster stage. For a large fuel burn-up $\varepsilon \sim 100\,p_{max}$, and with $p_{max} = (1/2)\,\varrho_p v_p^2$, we find that

$$v_p'/v_p \cong 10\,. \tag{3.2}$$

Therefore, if $v_p \sim 40$ km/sec, then $v_p' \cong 400$ km/sec, and which would be more than enough to make impact fusion work.

For two 4 cm steel projectiles driving the booster stage at a mutual impact velocity of ~ 20 km/sec, the kinetic input energy is ~ 200 MJ. The energy going into black body radiation is 4.5 MJ. With a gain of ~ 600 in the high gain stage of a Bangerter type target, the energy output would be 2700 MJ. Compared with the energy input from the projectiles, the overall gain would be therefore only ~ 13. However, much larger overall gains are possible by staging [14], whereby the energy released from a smaller high gain microexplosion would set off a second much larger microexplosion. Similar multistage arrangements which are possible for ablatively-driven targets, are of course also possible for impact fusion targets.

With multistage targets, the final yields may be very high. However, because projectile-initiated microexplosions permit a large stand-off distance in between the microexplosion and the reactor wall, this therefore should pose no principal problem. If the thusly ignited microexplosions are used for rocket propulsion, large overall yields are even desired.

4. Magnetic Acceleration

A velocity of a few 10 km/sec can possibly be reached by magnetic propulsion techniques which are suitable to accelerate large masses. The mag-

netic acceleration method works through the gradient of a magnetic pressure force. Consider a conducting projectile of cross section S, length h and density ϱ, placed in an inhomogeneous magnetic field. If the conductivity of the projectile is high, it excludes the magnetic field. Then, if the magnetic field at the back side of the projectile is $H > 0$ but falls off to $H \cong 0$ at its front side, that is if the axial field gradient is $\sim H/h$, the magnetic pressure force acting on its backside is $F = S\,(H^2/8\,\pi)$, and the equation of motion of the projectile is given by

$$m\,\ddot{z} = S\,(H^2/8\,\pi)\,, \tag{4.1}$$

where the z-coordinate is directed along h, and where the projectile mass is $m = S\,h\,\varrho$. Hence

$$\ddot{z} = H^2/8\,\pi\,\varrho\,h\,. \tag{4.2}$$

If $H = \text{const}$, the length L of the accelerator to reach a velocity v is given by

$$L = 4\,\pi\,\varrho\,v^2\,h/H^2\,. \tag{4.3}$$

The magnetic pressure $H^2/8\,\pi$ acting on the projectile must be less than the tensile strength σ of the projectile material. Putting $H^2/8\,\pi < \sigma$ into (4.3) we recover (1.2). For $\sigma \cong 10^{10}\,\text{dyn/cm}^2$ we find that $H \lesssim 5 \times 10^5\,\text{G}$. Therefore, if $H \cong 5 \times 10^5\,\text{G}$ can be reached, the combined length of two magnetic accelerators launching two projectiles with $\sim 20\,\text{km/sec}$ is ~ 100 meters.

The different magnetic acceleration methods have been reviewed by Ribe and Peaslee [15]. To reach very high velocities, the projectile cannot be in contact with the wall of the accelerating tube, and also is not subjected to dissipative electric currents. The fulfillment of the first of these two conditions requires the elimination of wall friction, and the second of Ohmic heating. A projectile accelerator meeting both these conditions is the magnetic dipole travelling wave accelerator with either superconducting or ferromagnetic projectiles. However, because a field strength of $\sim 5 \times 10^5\,\text{G}$ can in this case not be easily realized, the accelerator length is there much larger than ~ 100 meters.

Larger accelerations and hence shorter accelerators are possible with railguns, but since here the projectile is in physical contact with the wall the attainable velocities are smaller. At high velocities, the most serious loss mechanism result from friction followed by radiation. To estimate this loss effect consider a projectile of rectangular cross section D^2, with a clearance δ from the wall of the accelerator tube. The radiative energy flux produced by the friction losses with the wall, and which passes through the area $4\,D\,\delta$, is given by

$$\Phi_\text{r} = 4\,D\,\delta\,\varkappa\,T_\text{a}^4\,, \tag{4.4}$$

where T_a is the adiabatic wall temperature on the wall and projectile surface of a plasma formed in between both, and where $\varkappa = 5.75 \times 10^{-5}\,\text{erg/cm}^2\,\text{sec}\,\text{K}^4$ is the Stefan Boltzmann constant. The power to drive the projectile is

$$\Phi_\text{p} = (H^2/8\,\pi)\,D^2\,v \lesssim \sigma\,D^2\,v\,, \tag{4.5}$$

and which has to be equated with Φ_r. If we equate Φ with Φ_r we can get an estimate for the upper velocity above which the radiation losses become prohibitive.

The adiabatic wall temperature is given by [16]

$$T_\text{a} = \sqrt{P}\,v^2/2\,c_p\,, \tag{4.6}$$

where P is the Prandtl-number and c_p the specific heat at constant pressure. For a singly ionized plasma one finds

$$T_\text{a} \cong 3.4 \times 10^{-9} A\,v^2/(Z+1)\,, \tag{4.7}$$

where A is the atomic weight and Z the degree of ionization. Equating Φ_p with Φ_r, eliminating T_a by (4.7) and solving for v, one finds

$$v \cong 2.3 \times 10^5\,(\sigma\,D/\delta)^{1/7}\,((Z+1)/A)^{4/7}\,. \tag{4.8}$$

Putting $\sigma = 10^{10}\,\text{dyn/cm}^2$, $D/\delta \cong 10$, and $(Z+1)/A \cong 0.1$, one finds $v \cong 23\,\text{km/sec}$. Larger velocities are possible with larger values of Z/A. This suggests to put a hydrogen plasma in between the projectile and wall. The value $(Z+1)/A \cong 0.1$ may be considered more typical for plasmas produced by erosion from the projectile or wall. For a hydrogen plasma $(Z+1)/A = 2$ and $v \cong 130\,\text{km/sec}$.

The limitation by the other loss mechanism, resulting from the resistive losses of the electric current passing through the projectile, can be also easily estimated. From the magnetic force density ($\boldsymbol{j}$ electric current density in esu)

$$\boldsymbol{f} = \frac{1}{c}\,\boldsymbol{j} \times \boldsymbol{H} \tag{4.9}$$

and Maxwell's equation

$$\frac{4\,\pi}{c}\,j = \text{curl}\,\boldsymbol{H}\,, \tag{4.10}$$

follows by order of magnitude

$$f \cong (4\pi\, l/c^2)\, j^2\,, \tag{4.11}$$

where l is the linear dimension of the conducting projectile. The resistive energy losses are given by

$$\varepsilon = j^2/\sigma_e\,, \tag{4.12}$$

where σ_e is the electrical conductivity of the projectile. From the equation of motion (a = acceleration):

$$\varrho\, a = f \tag{4.13}$$

and the equation:

$$\varrho\, C T_m = \varepsilon\, t_m\,, \tag{4.14}$$

where C is the specific heat of the projectile material, T_m its melting temperature, and t_m the acceleration time at which the projectile melts, one can calculate the maximum attainable velocity under the assumption of a more or less uniform current distribution inside the projectile. One has

$$a = f/\varrho = 4\pi\, l\, j^2/\varrho\, c^2 \tag{4.15}$$

and

$$v = a\, t_m = a\, (\varrho\, C T_m/\varepsilon)\,, \tag{4.16}$$

hence

$$v = 4\pi\, l\, C T_m\, \sigma_e/c_2\,. \tag{4.17}$$

We note that this maximum velocity does not depend upon j. We take the example $C T_m \cong 10^9$ erg/g, $\sigma_e \cong 10^{17}\,\mathrm{sec}^{-1}$, $l = 4$ cm, and find $v \cong 55$ km/sec.

Rather than directly accelerating a projectile by currents flowing through it, one may instead accelerate it indirectly by the pressure from a plasma which in turn is magnetically accelerated. This concept permits to accelerate even a nonconducting projectile. In case a hydrogen plasma is used to drive the projectile, the above given upper velocity estimate of ~ 100 km/sec applies. This idea appears to have first been proposed in 1964 by Brast and Sawle [17], using a railgun accelerator. More recently the idea has been greatly developed by Rashleigh and Marshall [18] and by Hawke [19]. The principle of such a railgun accelerator is shown in Figure 3. The current I, flowing along the rails produces an electric arc, and the magnetic field produced by the current pushes the arc, and the arc plasma pushes the projectile positioned in front of the arc.

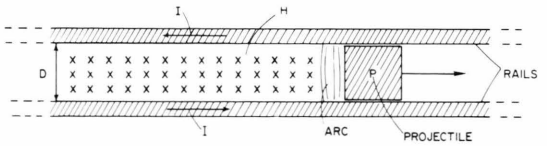

Fig. 3. Railgun accelerator with arc armature.

If the separation between the rails is D, the magnetic field in between is given by (I measured in ampere):

$$H = 0.4\pi\, D/I\,. \tag{4.18}$$

To produce $H = 5 \times 10^5$ G, the upper value consistent with the tensile strength of the projectile, this would require $I \cong 5 \times 10^5 A$, assuming that $D \sim 1$ cm. A current of this magnitude can be drawn from a homopolar generator, or from an inductive energy storage device, for example of the kind developed by Cowan et al. [20].

More recently a novel kind of macroparticle accelerator, called electromagnetic rocket gun, has been proposed by the author [21]. In this concept, the projectile to be accelerated by a travelling magnetic wave is at the same time a rocket, preferably using a hydrogen propellant. There the hydrogen propellant not only cools the projectile and prevents its vaporization, but it also substantially increases the thrust through the heating of the propellant jet by the travelling magnetic wave. With this concept, the required velocities could be easily reached.

5. Fluid Dynamic Acceleration by Imploding Shells

The fluid dynamic acceleration method makes use of two facts, first that a velocity up to 10 km/sec can be already reached with purely ballistic methods using light gas guns, and second, that a further acceleration to a velocity 20 km/sec can from there on be reached by shell implosions receiving their initial implosion velocity from light gas gun fired projectiles. A light gas gun is a two stage gun, where in the first stage a chemical propellant drives a piston. The piston isentropically compresses and heats a hydrogen gas to a high temperature, and which thereafter acts as a propellant to drive a second stage projectile attaining a much higher velocity than the piston of the first stage.

Several light gas guns can then be arranged around the shell to be imploded by the simultaneous firing of several projectiles. This configuration is shown schematically in Figure 4. For a cylindrical shell implosion the guns are arranged in a circle, and for a spherical implosion they are arranged on spherical surface.

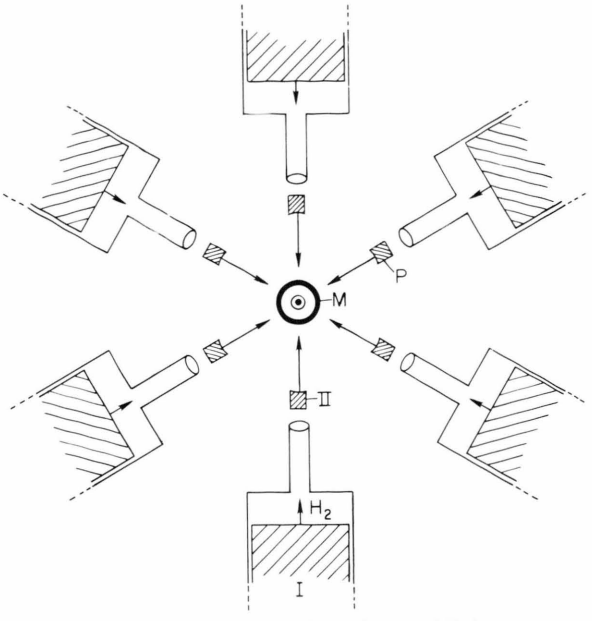

Fig. 4. Shell M imploded by action of several light gas gun fired projectiles P. I first light gas gun stage, II second stage.

If the shell material is incompressible, the shell implosion problem is similar to the classical cavitation problem by Rayleigh. This theory predicts an inner wall velocity at the distance R near the center of implosion given by

$$v \cong \frac{v_0}{\sqrt{2}}\left(\frac{R_0}{R}\right)\left(\log\left(\frac{R_0}{R}\right)\right)^{-1/2} \quad \text{cylinder}, \quad (5.1)$$

$$v \cong \frac{v_0}{\sqrt{3}}\left(\frac{R_0}{R}\right)^{3/2} \quad \text{sphere}. \quad (5.2)$$

In these equations, R_0 is the initial inner shell radius and v_0 the externally applied velocity. The increase in the velocity at the inner shell surface is the result of the fattening of an incompressible shell during its implosion as shown in Fig. 5, by which the velocity at the inner surface can become much larger than the velocity at its outer surface. If $v_0 \cong 10$ km/sec, attainable with light gas guns, and if $v = 20$ km/sec shall be reached, corresponding to a mutual velocity of opposite sides of the collapsing cavity wall equal to 40 km/sec, one computes that $R_0/R \cong 2.8$ for a cylindrical and $R_0/R \cong 2.3$ for a spherical implosion. However, as we had seen above, for velocities in excess of

$$v \cong (2/\varrho\varkappa)^{-1/2}, \quad (5.3)$$

where $\varkappa$ is the compressibility of the shell material, the incompressibility assumption becomes invalid. For steel it was estimated that this will happen for velocities in excess of 8 km/sec. Using light gas gun fired projectiles with a velocity of ~ 10 km/sec, the corresponding expressions for compressible shells have to be derived. Applying Guderley's method [22] to obtain selfsimilar solutions, the problem was solved by Hunter [23] in the context of the cavitation problem in water for spherical implosions, using as equation of state of the form given by (2.18) and assuming that $\gamma = 7$. We follow the same procedure but extend it to a wide range of γ-values and in addition also treat the case of cylindrical shell implosions. We make the assumption that $\gamma = \text{const}$, even though in reality γ depends upon the pressure. This simplifying assumption permits to obtain selfsimilar solutions. If these solutions are

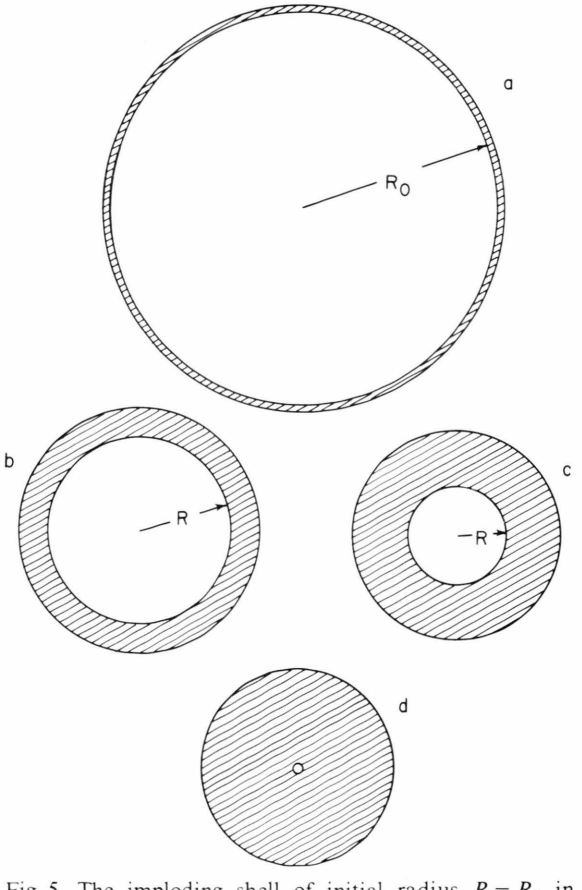

Fig. 5. The imploding shell of initial radius $R = R_0$ in its initial configuration (a), and three consecutive stages, (b), (c) and (d), during its implosion.

known for a wide range of γ-values, a good estimate can be made about the rise in velocity in any practical situation, provided the value of γ is known for a given value of the pressure.

With the parameter s, which for $s=1$ represents the cylindrical and for $s=2$ the spherical shell implosion case, the fluid dynamic equations in cylindrical or spherical coordinates are:

momentum:

$$\frac{\partial v}{\partial t}+v\frac{\partial v}{\partial r}+\frac{1}{\varrho}\frac{\partial p}{\partial r}=0\,, \tag{5.4}$$

continuity:

$$\frac{\partial \varrho}{\partial t}+v\frac{\partial \varrho}{\partial r}+\varrho\left(\frac{\partial v}{\partial r}+s\frac{v}{r}\right)=0\,. \tag{5.5}$$

In (5.4) and (5.5) v is the radial implosion velocity at the radial coordinate inside the shell, and ϱ the variable shell density, with a dependence $\varrho=\varrho(p)$ given by (2.18). With the help of (2.18) we have for the velocity of sound c:

$$c^2=\frac{\mathrm{d}p}{\mathrm{d}\varrho}=A\,\varrho^{\gamma-1}\,. \tag{5.6}$$

Equations (5.4) and (5.5) can then be written as follows:

$$\frac{\partial v}{\partial t}+v\frac{\partial v}{\partial r}+\frac{1}{\gamma-1}\frac{\partial c^2}{\partial r}=0\,, \tag{5.7}$$

$$\frac{\partial c^2}{\partial t}+v\frac{\partial c^2}{\partial r}+(\gamma-1)\,c^2\left(\frac{\partial v}{\partial r}+s\frac{v}{r}\right)=0\,. \tag{5.8}$$

To solve these equations we introduce the similarity variable ξ defined by

$$\xi=-\left(\frac{R}{r}\right)^{1/n}=\frac{\alpha\,t}{r^{1/n}}\,,\qquad \alpha=\text{const}\,, \tag{5.9}$$

where R is the radius of the inner surface of the collapsing shell and for which $\xi=-1$. The r-axis has the value $\xi=0$. In (5.9) n is called the homology exponent. From (5.9) it follows that

$$R=(-\alpha\,t)^n \tag{5.10}$$

and

$$\dot{R}=-n\,\alpha\,R^{1-1/n}\,. \tag{5.11}$$

According to Guderley the homology exponent n can be obtained from a regularity condition at a singular point of a nonlinear differential equation derived from the gas dynamic equations under the homology assumption. The only independent parameter in the gas dynamic equations is the specific heat ratio γ. We therefore can conclude that for the regular solutions $n=n(\gamma)$. The knowledge of this function gives us the implosion velocity in the limiting case $R\to 0$, by inserting the value of n into (5.11).

We now look for solutions of the form

$$\begin{aligned} v&=-n\,\alpha\,r^{1-1/n}\,F(\xi)\,,\\ c^2&=n^2\,\alpha^2\,r^{2-2/n}\,G(\xi)\,. \end{aligned} \tag{5.12}$$

If we insert (5.12) into (5.7) and (5.8), the dependence upon r drops out and we find two coupled ordinary differential equations for the functions $F(\xi)$ and $G(\xi)$:

$$\begin{aligned}&(\gamma-1)\,(1+\xi\,F)\,F'+\xi\,G'\\ &\qquad+(1+n)\,((\gamma-1)\,F\gamma+2G)=0\,,\end{aligned} \tag{5.13}$$

$$\begin{aligned}&(\gamma-1)\,\xi\,G\,F'+(1+\xi\,F)\,G'\\ &\qquad+[(1-n)\,(\gamma+1)-s\,(\gamma-1)\,n]\,F\,G=0\,.\end{aligned} \tag{5.14}$$

Here $F'\equiv \mathrm{d}F/\mathrm{d}\xi$ and $G'\equiv \mathrm{d}G/\mathrm{d}\xi$. From (5.11) and (5.12) it follows that the boundary condition for F at the cavity wall, where $\xi=-1$, is $F=1$. The other boundary condition $G=0$ at $\xi=-1$ follows from the fact that the pressure at the cavity wall is zero and hence $c=0$.

Next we make a change of variables by the following transformation

$$\begin{aligned} x&=\ln(-\xi)\,,\\ y&=-\xi\,F\,,\\ z&=\xi^2\,G\,. \end{aligned} \tag{5.15}$$

Expressed in these variables one has $x=\ln 1=0$ at the cavity wall, with (5.13) and (5.14) taking the following compact form:

$$\begin{aligned}&\mathrm{d}x:\mathrm{d}y:\mathrm{d}z=[(y-1)^2-z]\\ &:\left[y\,(y-1)\,(n\,y-1)-(s+1)\,n\,y\,z+\frac{2\,(1-n)}{\gamma-1}\,z\right]\\ &:\left[2z\left[-n\,z+\frac{n\,y^2}{2}\,((2-s)+s\,\gamma)\right.\right.\\ &\qquad\left.\left.+\frac{y}{2}\,(\gamma-3-((s+1)\,\gamma+1-s)\,n)+1\right]\right]\,.\end{aligned} \tag{5.16}$$

Of these three differential equations, only two are independent. One of them however, contains two

variables only, and it thus is separated from the other two. This differential equation is

$$\frac{dy}{dz}=\left[y(y-1)(ny-1)-(s+1)nyz+\frac{2(1-n)}{\gamma-1}z\right] : \left[2z\left[-nz+\frac{ny^2}{2}((2-s)+s\gamma) + \frac{y}{2}(\gamma-3-((s+1)\gamma+1-s)n)+1\right]\right] \tag{5.17}$$

In the limiting case where the r.h.s. of (5.20) is set equal to the l.h.s., one obtains a quadratic equation for n. In solving this quadratic equation for n, we have to take the positive sign of the root to discard solutions which give a velocity rise faster than in the incompressible case if $R \to 0$. Calling the obtained value of $n = n_{\min}$, we have for a cylinder where $s = 1$,

$$n_{\min}=\frac{\gamma^2-3\gamma+4+[(\gamma^2-3\gamma+4)^2-(\gamma-3)^2(\gamma^2-2\gamma+2)]^{1/2}}{2\gamma^2-4\gamma+4} \tag{5.21}$$

and for a sphere where $s = 2$

$$n_{\min}=\frac{3\gamma^2-6\gamma+7+[(3\gamma^2-6\gamma+7)^2-(\gamma-3)^2(9\gamma^2-14\gamma+9)]^{1/2}}{9\gamma^2-14\gamma+9}. \tag{5.22}$$

and from which the value of n can be determined under the condition that the solution is regular in passing through a singular point. A differential equation is singular if both its numerator and denominator vanish. For the regularity of the solution only one singular point is of importance. It is positioned on the parabola

$$z=(y-1)^2. \tag{5.18}$$

According to (5.16) both dx/dy and dx/dz vanish on this parabola. On the singular point one has $d\xi/dF = d\xi/dG = 0$. This means the function ξ has there a turning point. From the existence of such a turning point follows that F and G are not single-valued functions of ξ for an integral curve passing through such a point in the $y-z$ plane, and an integral curve of this kind cannot be physically relevant. There is however, one particular integral curve belonging to a particular value of n which does not have a turning point in passing through this singularity. It is this particular solution which determines n.

A lower limit for n can be obtained by inserting the function (5.18) into the denominator of (5.17) and which is set equal to zero:

$$s(\gamma-1)ny^2-((s+1)(\gamma-1)n-(\gamma-1)+2(1-n))y+2(1-n)=0. \tag{5.19}$$

Equation (5.19) has a real solution if

$$((s+1)(\gamma-1)n-(\gamma-1)+2(1-n))^2 \geqq 8s(\gamma-1)n(1-n). \tag{5.20}$$

In the limit $\gamma \to \infty$, one obtains

$$n_{\min}=\begin{cases}1/2 & \text{cylinder},\\ 1/3 & \text{sphere}.\end{cases} \tag{5.23}$$

To obtain the exact value of n, the differential equation (5.17) has to be integrated from $\xi = -1$ to $\xi = 0$ that is from $F = 1$, $G = 0$ to $F = G = 0$, or from $y = 1$, $z = 0$ to $y = z = 0$. In the numerical integration which was done with the Runge-Kutta method we inserted in the first run $n = n_{\min}$ and thereafter increased n in small steps until the turning point, where the integral curve crosses parabola (5.18), vanishes. This thusly found value of $n = n(\gamma)$ is the solution of the problem.

For the cylindrical case the differential equation is

$$\frac{dy}{dz}=\left[y(y-1)(ny-1)-2nyz+\frac{2(1-n)}{\gamma-1}z\right] : \left[2z\left[-nz+\frac{\gamma+1}{2}ny^2+\frac{y}{2}(\gamma-3-2\gamma n)+1\right]\right] \tag{5.24}$$

and for the spherical case

$$\frac{dy}{dz}=\left[y(y-1)(ny-1)-3nyz+\frac{2(1-n)}{\gamma-1}z\right] : \left[2z\left[-nz+n\gamma y^2+\frac{y}{2}(\gamma-3-(3\gamma-1)n)+1\right]\right] \tag{5.25}$$

Introducing the quantity $m = 1/n - 1$, the implosion velocity in the vicinity $R \to 0$ is given by

$$v = \text{const}\, R^{-m}. \tag{5.26}$$

Table 2.

	Cylinder		Sphere	
γ	n	m	n	m
5/3			0.92	0.087
2			0.835	0.198
3	0.88	0.14	0.71	0.409
4	0.82	0.22	0.64	0.563
5	0.775	0.29	0.60	0.667
6	0.75	0.34	0.574	0.742
7	0.73	0.375	0.5544	0.804
8	0.71	0.41	0.5407	0.8495
9	0.70	0.43	0.5294	0.8889
10	0.69	0.45	0.5198	0.9238
11	0.68	0.47	0.5115	0.9549
12	0.67	0.49	0.5043	0.9830
13	0.67	0.50	0.4979	1.0085
14	0.66	0.51	0.4922	1.0318
15	0.655	0.53	0.4870	1.0533
16	0.65	0.54	0.4824	1.0732
17	0.65	0.54	0.4781	1.0916
18	0.64	0.56	0.4742	1.1089
19	0.64	0.56	0.4706	1.125
20	0.64	0.56	0.4673	1.1402

This expression can be used to estimate the rise in the inner wall velocity after $m = m(\gamma)$ has been determined by the numerical integration of (5.17). In Table 2 we have compiled the results of the numerical integration, both for the cylindrical and spherical case. In Fig. 6 the functions $n(\gamma)$ $n_{\min}(\gamma)$ and $m(\gamma)$ are displayed for the cylindrical and in Fig. 7 for the spherical case. From these results it can be seen that for sufficiently large values of γ, n rapidly approaches the limit $n_{\min}$. For $\gamma \to \infty$, the implosion velocity is therefore given by

$$v = \begin{cases} \text{const } R^{-1} & \text{cylinder}, \\ \text{const } R^{-2} & \text{sphere}. \end{cases} \tag{5.27}$$

A typical value at megabar pressures is $\gamma \cong 10$, but at the higher pressures considered here, the value $\gamma \cong 4$, obtained from high explosive experiments, may be a better approximation. For $\gamma = 4$, the velocity rise is given by

$$v = \begin{cases} \text{const } R^{-0.22} & \text{cylinder}, \\ \text{const } R^{-0.56} & \text{sphere}. \end{cases} \tag{5.28}$$

Therefore, to obtain a twofold rise in the velocity, to go from $v_0 \cong 10$ km/sec to $v \cong 20$ km/sec, requires to make $R_0/R \cong 22$ for the cylindrical case, and $R_0/R \cong 3.4$, for the spherical case.

Applied to the booster stage concept, this result has the following implication. The booster stage needs an implosion velocity $v_{\text{imp}} \cong 20$ km/sec, reached at a distance $l_{\min} = 0.4$ cm. The length $l_{\min}$ has to be set equal to the radius R where $v = 20$ km/sec. With an initial velocity of ~ 10 km/sec, the initial shell radius would be $R_0 \cong 9$ cm in case of a cylindrical, and $R_0 \cong 1.4$ cm in case of a spherical implosion.

The spherical implosion seems to have a clear advantage over a cylindrical implosion, but in case several magnetic guns are used, producing a velocity just somewhat larger than those to be attainable with light gas guns, a cylindrical implosion could also work with a smaller initial shell radius. This

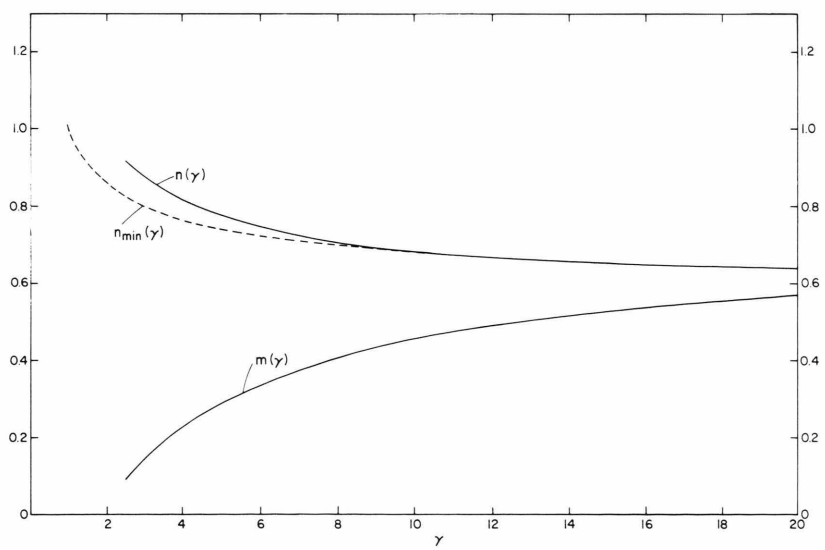

Fig. 6.
The functions $n(\gamma)$, $n_{\min}(\gamma)$ and $m(\gamma)$ for the cylindrical shell implosion.

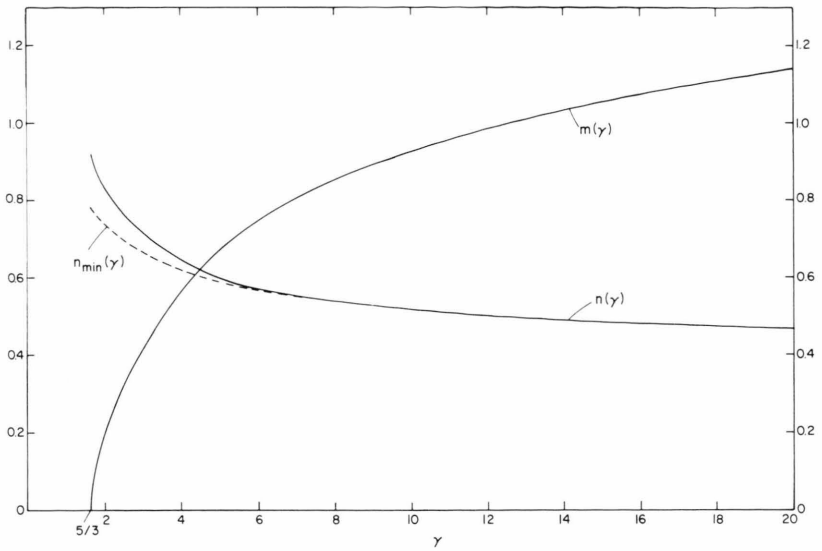

Fig. 7.
The functions, $n(\gamma)$, $n_{\min}(\gamma)$ and $m(\gamma)$ for the spherical shell implosion.

would have the advantage that the guns can here be arranged in a plane positioned on a circle.

The imploded shell must be sufficiently fat, to assure that the inertial confinement time for the booster stage is long enough. This means that the outer radius of the imploded shell must be of the order $h \cong 4$ cm, with a volume of the imploded shell about $\sim 250\,\text{cm}^3$. At a density $\varrho \sim 7\,\text{g/cm}^3$ and an initial velocity of 10 km/sec, the kinetic energy of the shell would be $\sim 10^{15}$ erg = 100 MJ. This comparatively large energy input shows that one has to pay a price if fluid dynamic acceleration methods are used. One reason is that in the fluid dynamic acceleration a large portion of the energy goes into compression of the shell rather than kinetic energy. An optimal configuration might therefore combine magnetic propulsion and shell implosion techniques.

Instead of light gas gun fired projectiles, one can implode the shells by chemical high explosives. However, because there initial implosion velocities of only ~ 3 km/sec are possible, this approach requires larger shells. Using chemically induced shell implosions to drive a booster stage appears less attractive for reactor applications but could be used for rocket propulsion, which will be discussed elsewhere.

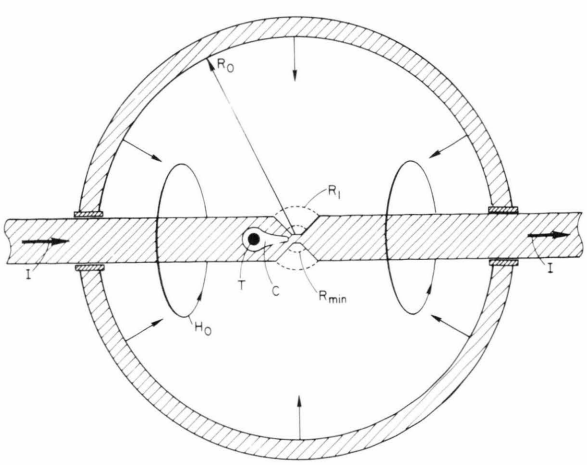

Fig. 8. Combination of imploding shell and magnetic booster target. I and H_0 initial current and magnetic field. C cavity containing high yield target T.

6. Special Configurations Combining Shell Implosion with Booster Stage Concept

In the configuration shown in Fig. 8, the shell is penetrated by a conducting rod which is electrically insulated against the shell. A current drawn from a capacitorbank and flowing through the conducting rod, produces the initial azimuthal magnetic field, which after being imploded and amplified, becomes the initial field of the booster stage. Near the center where it narrows, the rod contains a small cavity and into which the high gain second stage target is placed. The space in between the conducting rod and the inner shell surface is filled with DT gas.

Shortly after the beginning of the implosion the current through the rod is crowbarred by the im-

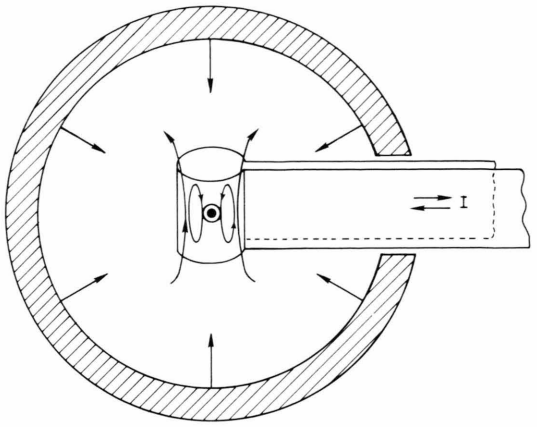

Fig. 9. Field reversed θ-pinch booster target driven by imploding shell.

ploding shell at the two positions where the conducting rod passes through the shell. The return current thereafter goes through the shell but also through the DT plasma, if in the meantime a plasma is formed in the space inside the shell. If the shell is a good conductor the magnetic field is trapped inside the shell and rises as R^{-2}, with the magnetic pressure rising as R^{-4}. The shell stagnation pressure by comparison, rises much more slowly. In case of the $R^{-0.6}$ law the pressure rises as $R^{-1.2}$. One therefore can always choose the initial conditions in such a way that the magnetic pressure brings the implosion to a halt at a smallest radius $R = R_{\min}$.

For thusly chosen initial conditions the effect of the magnetic pressure on the implosion process can in first approximation be neglected. The same is true for the pressure of the DT plasma inside the imploding cavity, since for an isentropic compression with a specific heat ratio $\gamma = 5/3$, the plasma pressure rises as R^{-5}. Ideally, the initial conditions are chosen in such a way to make at $R = R_{\min}$, first, the sum of the magnetic and plasma pressure equal the shell stagnation pressure, and second, the magnetic pressure equal the plasma pressure. If the magnetic and plasma pressure are equal, the DT plasma becomes thermally insulated as in the case of magnetic confinement.

The configuration used in this magnetic booster stage resembles the belt pinch of ordinary magnetic confinement fusion devices. One, of course, can also choose from many other different magnetic confinement configurations. Figure 9 for example, shows a booster stage using a field reversed θ-pinch generated inside a small oneturn coil. To achieve field reversal the current direction has to be changed during the discharge. Inside the θ-pinch coil is positioned a small shell containing the second stage high yield target. After the imploding shell has compressed and ignited the θ-pinch plasma, a thermonuclear excursion takes place as before. The inner shell containing the second stage high yield target vaporizes and the second stage target is bombarded by black body radiation.

[1] F. Winterberg, in: Physics of High Energy Density, Academic Press, New York 1971, p. 376ff.
[2] F. Winterberg, Nature London **286,** 60 (1980).
[3] F. Winterberg, Z. Physik A **296,** 3 (1980).
[4] F. Winterberg, Atomkernenergie **36,** 226 (1980).
[5] F. Winterberg, Atomkernenergie **38,** 81 (1981).
[6] F. Winterberg, The Physical Principles of Thermonuclear Explosive Devices, Fusion Energy Foundation, New York 1981, p. 125ff.
[7] J. Chang et al., Proceedings of the 2nd International Topical Conference on High Power Electron and Ion Beam Research and Technology, Oct. 3–5, 1977, Cornell University Ithaca, New York.
[8] J. G. Linhart, Nuclear Fusion **10,** 211 (1970).
[9] F. Ribe and G. C. Vlases, Proceedings of the Impact Fusion Workshop, July 10–12, 1979, Los Alamos, LA-8000-C, page 2.
[10] Ya. B. Zeldovich and Ya. P. Raizer, Physics of Shock Waves and High Temperature Hydrodynamic Phenomena, Vol. II, Academic Press, New York 1967, page 710.
[11] L. D. Landau and E. M. Lifshitz, Fluid Mechanics, Pergamon Press, London 1959, p. 27–29.
[12] M. Schwarzschild, Structure and Evolution of Stars, p. 67ff., Princeton University Press 1958.
[13] R. O. Bangerter, Energy and Technology Review, March 1980 and UCRL-52000-80-3.
[14] F. Winterberg, Nature, London **258,** 512 (1975), and J. Plasma Physics **16,** 81 (1976).
[15] F. L. Ribe and A. T. Peaslee, Jr. Final Report: Evolution of Impact Fusion Concepts, Fusion Plasma Program, University of Washington, January 30, 1980.
[16] H. Schlichting, Boundary Layer Theory, McGraw-Hill, New York 1968, page 318.
[17] D. E. Brast and D. R. Sawle, Proceedings of the 7th Symposium on Hypervelocity Impact, Tampa Florida 1964. Orlando Florida: Martin Company 1965.
[18] S. C. Rashleigh and R. A. Martin, J. Appl. Phys. **49,** 2540 (1978).
[19] R. S. Hawke, Atomkernenergie **38,** 35 (1981).
[20] M. Cowan, E. C. Cnare, W. B. Leisher, W. K. Tucker, and D. L. Wesenberg, Cryogenics, December 1976, page 699ff.
[21] F. Winterberg, Atomkernenergie/Kerntechnik **43,** 104 (1983).
[22] G. Guderley, Luftfahrtforschung **19,** 302 (1942).
[23] C. Hunter, J. Fluid Mechanics **8,** 241 (1960).